RHEUMATOLOGY

Original article

doi:10.1093/rheumatology/kex280

Scleroderma keratinocytes promote fibroblast activation independent of transforming growth factor beta

Sara S. McCoy[1], Tamra J. Reed[2], Celine C. Berthier[3], Pei-Suen Tsou[2], Jianhua Liu[2], Johann E. Gudjonsson[4], Dinesh Khanna[2] and J. Michelle Kahlenberg[2]

Abstract

Objectives. SSc is a devastating disease that results in fibrosis of the skin and other organs. Fibroblasts are a key driver of the fibrotic process through deposition of extracellular matrix. The mechanisms by which fibroblasts are induced to become pro-fibrotic remain unclear. Thus, we examined the ability of SSc keratinocytes to promote fibroblast activation and the source of this effect.

Methods. Keratinocytes were isolated from skin biopsies of 9 lcSSc, 10 dcSSc and 13 control patients. Conditioned media was saved from the cultures. Normal fresh primary fibroblasts were exposed to healthy control and SSc keratinocyte conditioned media in the presence or absence of neutralizing antibodies for TGF-β. Gene expression was assessed by microarrays and real-time PCR. Immunocytochemistry was performed for α-smooth muscle actin (α-SMA), collagen type 1 (COL1A1) and CCL5 expression.

Results. SSc keratinocyte conditioned media promoted fibroblast activation, characterized by increased α-SMA and COL1A1 mRNA and protein expression. This effect was independent of TGF-β. Microarray analysis identified upregulation of nuclear factor κB (NF-κB) and downregulation of peroxisome proliferator-activated receptor γ (PPAR-γ) pathways in both SSc subtypes. Scleroderma keratinocytes exhibited increased expression of NF-κB-regulated cytokines and chemokines and lesional skin staining confirmed upregulation of CCL5 in basal keratinocytes.

Conclusion. Scleroderma keratinocytes promote the activation of fibroblasts in a TGF-β-independent manner and demonstrate an imbalance in NF-κB1 and PPAR-γ expression leading to increased cytokine and CCL5 production. Further study of keratinocyte mediators of fibrosis, including CCL5, may provide novel targets for skin fibrosis therapy.

Key words: scleroderma, keratinocyte, fibroblast, TGF-β, CCL5, NF-κB, PPAR-γ

CLINICAL SCIENCE

Rheumatology key messages

- Keratinocytes from scleroderma patients participate in fibroblast activation.
- Normal and SSc keratinocytes do not secrete TGF-β.
- Upregulation of NF-κB1 and downregulation of PPAR-γ pathways correlate with scleroderma skin scores.

[1]Department of Internal Medicine, Division of Rheumatology, University of Wisconsin, Madison, WI, [2]Department of Internal Medicine, Division of Rheumatology, [3]Department of Internal Medicine, Division of Nephrology, and [4]Department of Dermatology, University of Michigan, Ann Arbor, MI, USA

Submitted 5 December 2016; revised version accepted 12 June 2017

*Correspondence to: J. Michelle Kahlenberg, 5570A MSRB II, 1150 W. Medical Center Drive, Ann Arbor, MI 48109-5678, USA. E-mail:mkahlenb@med.umich.edu

Introduction

SSc is a rare but devastating disease of fibrosis affecting the dermis and multiple organ systems. The prevalence ranges from 4 to 489 cases per million individuals [1, 2], with 10-year mortality rates reported as ~18% [3]. SSc can be subclassified as lcSSc, defined by involvement of skin sclerosis restricted to distal to the elbows and knees, and dcSSc, defined by extensive skin sclerosis extending

proximal to the elbows and knees. Survival is associated with the extent of skin involvement [4], yet the precise mechanisms driving skin fibrosis in SSc remain unknown.

SSc patients have increased collagen and extracellular matrix synthesis driven by fibroblast activation [5], which is characterized by transformation of fibroblasts to myofibroblasts. This is detected phenotypically by increased α-smooth muscle actin (α-SMA) expression and synthesis of collagen type 1 (COL1A1) [6]. Several factors have been implicated in myofibroblast differentiation, including TGF-β [7, 8], vascular endothelial growth factor [9], IL-13 activation of STAT6 [10] and toll-like receptor (TLR) ligands [11].

SSc skin has been found to express markers of inflammation and the epidermis has been a recent area of study. c-Rel, a subunit of nuclear factor κB (NF-κB), has been found to have abnormal expression in SSc keratinocytes; c-Rel null mouse models of bleomycin-induced skin fibrosis are protected [12]. Keratinocyte growth factor, which is increased in SSc fibroblasts, stimulates normal keratinocytes to secrete oncostatin M, which activates fibroblasts. Whole SSc epidermal sheets co-cultured with fibroblasts promote fibroblast contraction and expression of ET-1 and TGF-β, an effect mitigated by IL-1RA [13]. These data highlight the potential for crosstalk between keratinocytes and the dermis. In this study we evaluated the effects of lcSSc and dcSSc keratinocytes on fibroblast function in order to examine keratinocytes as a contributing factor to the pathogenesis of SSc.

Methods

Patient recruitment and keratinocyte acquisition

Procedures in this study were approved by the University of Michigan Medical Institutional Review Board (HUM00065044). Patients provided written consent to participate in the study. All subjects fulfilled 2013 ACR/EULAR criteria for SSc [14] and were subclassified as lcSSc and dcSSc based on Leroy criteria [15]. The demographic and clinical features of SSc and control patients are shown in supplementary Tables S1 and S2, available at *Rheumatology* Online. All skin biopsies were acquired via two 4 mm punch biopsies from the patients' non-dominant mid outer forearm 3–4 inches from the ulnar styloid. Local modified Rodnan skin score (MRSS) ranged from 1+ to 2+ for dcSSc biopsies and all lcSSc biopsies, except one that had an MRSS of 0. To isolate keratinocytes, the epidermis was separated from the dermis and incubated at 37 °C in basal media containing 0.17% trypsin for 2 h. Keratinocytes were initially selected in growth medium (EpiLife, Life Technologies, Grand Island, NY, USA) with keratinocyte growth factor supplementation (Life Technologies) and 2% foetal bovine serum (FBS; Sigma, St Louis, MO, USA) on 12 mm (24-well) Primera plates (BD, Franklin Lakes, NJ, USA). After 3 days, keratinocytes were switched to keratinocyte growth medium without FBS to prevent epithelialization and fibroblast contamination. Keratinocyte purity was confirmed via cellular morphology. Cells were passaged at 60% confluence, first onto a 6-well plate (p0) and then onto a 100 mm plate (p1). Three days after passage 2, conditioned media was collected and stored at −80 °C and 5 × 10^5 cells will be saved for RNA in Tripure (Roche, Basel, Switzerland).

Healthy control fibroblast culture conditions

Skin samples were obtained as above. The separated dermis was digested with 0.2% collagenase and grown in Roswell Park Memorial Institute (RPMI; Lonza, Walkersville, MD, USA) medium plus 10% FBS and 1% penicillin and streptomycin at 37 °C incubation. Fibroblasts were split 1:3 every 5 days. All fibroblasts were maintained in RPMI supplemented with penicillin (400 U/ml), streptomycin (50 mg/ml) and 10% FBS. All experiments were performed on fresh normal fibroblasts between passages 1 and 4. At 80% confluence, fibroblasts were serum starved for 24 h in RPMI with 1% FBS as previously described [16]. This was followed by incubation with 50% RPMI (1% FBS) and 50% keratinocyte conditioned media for 24 or 72 h. Fibroblasts treated with 10 ng/ml rhTGF-β served as the positive control for promotion of myofibroblast phenotype (Cell Signaling Technology, Danvers, MA, USA). Fibroblasts treated with keratinocyte growth media served as a negative control. For neutralization studies, the fibroblasts were incubated for 30 min with 2.5 μg/ml TGF-β antibody (R&D Systems, Minneapolis, MN, USA; clone 1D11) in RPMI in 1% FBS prior to stimulation with keratinocyte conditioned media.

Real-time quantitative PCR

Total RNA was purified using a Direct-Zol RNA kit (Zymo Research, Irvine, CA, USA). RNA was quantified utilizing a Nanodrop 2000 spectrophotometer (Thermo Fisher Scientific, Grand Island, NY, USA). One microgram of RNA was then transcribed to complementary DNA with oligo(dT) using a Peqlab (Wilmington, DE, USA) thermocycler. Real-time PCR was completed with the assistance of the University of Michigan DNA sequencing core on an ABI Prism 7900HT (Applied Biosystems, Waltham, MA, USA). Cycle times were normalized to beta-actin and graphed as fold-change expression over healthy keratinocytes using $2^{-\Delta\Delta CT}$.The primers used are as follows: α-SMA 5′-CGTG GGTGACGAAGCACAG-3 (forward) and 5′-CGTGGGTGACG AAGCACAG-3 (reverse); COL1 5′-AAGGTCATGCTGGTCTT GCT-3 (forward) and 5′-GACCCTGTTCACCTTTTCCA-3 (reverse); TNF-α 5′-TCCTTCAGACACCCTCAACC-3′ (forward) and 5′-AGGCCCCAGTTTGAATTCTT-3′ (reverse); TGF-β 5′-CAATTCCTGGCGATACCTCAG (forward) and 5′-GCACAAC TCCGGTGACATCAA-3′ (reverse); IL-1B 5′-ATGTCTGGAAC TTTGGCCATCTT-3′ (forward) and 5′-AGACAATTACAAAAG GCGAAGAAG ACT-3′ (reverse); IL-6 5′-ACTCACCTCTTCA GAACGAATTG-3′ (forward) and 5′-CCATCTTTGGAAGGTT CAGGTTG-3′ (reverse); CCL5 5′-CCAGCAGTCGTCTTTGTC AC-3′ (forward) and 5′-CTCTGGGTTGGCACACACTT-3′ (reverse); NF-κB1 5′-GAAGCACGAATGACAGAGGC-3′ (forward) and 5′-GCTTGGCGGATTAGCTCTTTT-3′ (reverse); PPAR-γ 5′-GGGATCAGCTCCGTGGATCT-3′ and 5′-TGCA CTTTGGTACTCTTGAAGTT-3′ (reverse); beta-actin 5′-CATC ACGATGCCAGTGGTACG-3′ (forward) and 5′-AACCGCGAG AAGATGACCCAG-3′ (reverse).

Fibroblast immunofluorescence

Primary fibroblasts were plated onto 8-well chamber slides (Fisher Scientific, Pittsburgh, PA, USA) and grown to 90% confluence. Serum starvation in RPMI with 1% FBS was performed for 24 h before stimulation for 72 h with 50% conditioned extracellular media isolated from dcSSc, lcSSc or control keratinocytes. Fibroblasts treated with 10 ng/ml rhTGF-β served as the positive control (Cell Signaling Technology). In TGF-β neutralizing experiments, 2.5 μg/ml TGF-β antibody (R&D Systems; clone 1D11) was added to fibroblasts 30 min before the keratinocyte conditioned media. Human IgG was utilized as an isotype control. After stimulation, cells were fixed in 4% formalin for 30 min at room temperature and then permeabilized with ice-cold methanol for 5 min at 4 °C. The cells were then blocked with 5% donkey serum and stained at room temperature for α-SMA expression using a well-defined polyclonal antibody [17] (Abcam, Cambridge, MA, USA) at a concentration of 2 μg/ml followed by staining with 5 μg/ml secondary FITC fluorescent conjugated antibody (Life Technologies) and counterstaining with 4′,6-diamidino-2-phenylindole (DAPI; BD Bioscience, San Jose, CA, USA). Fixed cells were imaged on an Olympus IX70 inverted fluorescent microscope (Olympus, Center Valley, PA, USA) with a 40× air objective. Illumination was provided by the X-cite series 120 metal halide light for fluorescence (EXFO, Mississauga, ON, Canada). FITC was measured with a 498 nm excitation and 520 nm emission filter and DAPI was measured using a 352 nm excitation and 461 nm emission filter. Optical filters were from Chroma Technology (Bellows Falls, VT, USA). Images were acquired by the CoolSNAP HQ2 camera (Photometrics, Tucson, AZ, USA) and recorded with MetaMorph software (Molecular Devices, Sunnyvale, CA, USA). At least 20 images were taken per slide. MetaMorph software was used to analyse all images. Shade and bias corrections were performed and the average background fluorescence was subtracted from the images. After correction, DAPI (nuclear stain) and FITC (α-SMA or TGF-β) images were combined into a red-green–blue overlay to allow for easy visualization of cells. A region was created that encompassed cells or a skin section of interest and defined the area to be measured. The DAPI image was used to record the number of nuclei using MetaMorph's Count Nuclei application. Integrated fluorescence values and areas were recorded for the FITC images. The mean immunofluorescence per cell was calculated by dividing the integrated fluorescence by the number of pixels (area) and dividing again for the number of nuclei in that region: mean immunofluorescence per cell = (integrated fluorescence/area)/number of cells.

Skin immunofluorescence

Paraffin-embedded preparations of normal skin and SSc tissue were incubated with 4% paraformaldehyde for 20 min, washed with PBS, then blocked with 10% donkey serum at room temperature for 1 h. Rabbit anti-human TGF-β primary antibody (Abcam) was applied at a 1:100 dilution for 12 h at 4 °C. The slides were washed and the FITC-labelled secondary antibody (Life Technologies) was added at a dilution of 1:400 for 1 h at room temperature. The slides were again washed with PBS and DAPI counterstaining was performed with Hoechst 1:200 dilution (BD Bioscience). Microscopy was performed and immunofluorescence was quantified through MetaMorph as discussed above.

Skin immunohistochemistry

Five micrometre frozen sections of SSc skin biopsies were obtained and utilized for CCL5 staining. The sections were baked at 37 °C for 1 h, fixed with 4% paraformaldehyde for 20 min and then boiled in 10 mmol/l citric acid buffer for 10 min for antigen retrieval. BLOXALL Blocking Solution (Vector Laboratories, Burlingame, CA, USA) was used to block endogenous peroxidase and alkaline phosphatase activities. CCL5 immunostaining was performed using an ImmPRESS Reagent Kit (anti-mouse IgG; Vector Laboratories). Briefly, the sections were blocked with normal goat serum for 30 min, then they were incubated overnight at 4 °C with primary mouse monoclonal anti-human CCL5/RANTES antibody (12.5 μg/ml) diluted in PBS containing 1% BSA (R&D Systems). Negative controls were incubated with the same concentration of matching IgG isotype. The reaction was visualized using an ImmPACT DAB Kit (Vector Laboratories). Sections were counterstained with haematoxylin (Thermo Fisher Scientific) and the slides were dehydrated in alcohol, cleared in xylene and mounted.

Supernatant cytokine measurement

Normal human and SSc keratinocytes were grown to 90% confluence in a 12-well plate. For measurement of TGF-β, keratinocyte cultures were stimulated with 5 μg/ml peptidoglycan, 1 μg/ml Polyl:C or 1 μg/ml lipopolysaccharide. Cells were stimulated for 24 h and culture media was saved for ELISA. TGF-β1 ELISA was performed per the manufacturer's instructions (eBioscience, San Diego, CA, USA).

Transcriptomic analyses

Transcriptomic analysis of keratinocytes was performed using Affymetrix ST2.1 GeneChips via the University of Michigan DNA Sequencing Core. The resulting CEL files passing the quality controls were from seven lcSSc, five dcSSc and seven normal skin samples. CEL files were normalized, log transformed, and analysed using ChipInspector software (Genomatix Software, Munich, Germany; www.genomatix.de) as previously described [18]. We used one class of exhaustive matching to detect the differentially regulated genes in the keratinocytes from diffuse fibrosis and limited skin disease compared with normal. We applied a false discovery rate of <1% on all datasets to detect the significantly regulated genes. A normalized data file was uploaded to the Gene Expression Omnibus website (http://www.ncbi.nlm.nih.gov/geo/) under accession number GSE81072 and will be available upon acceptance of this manuscript. Significantly regulated genes were analysed by creating biological literature-based networks using Genomatix Pathway System software. Canonical pathways were

Fig. 1 Fibroblast to myofibroblast conversion is increased in normal fibroblasts stimulated with SSc keratinocyte conditioned media

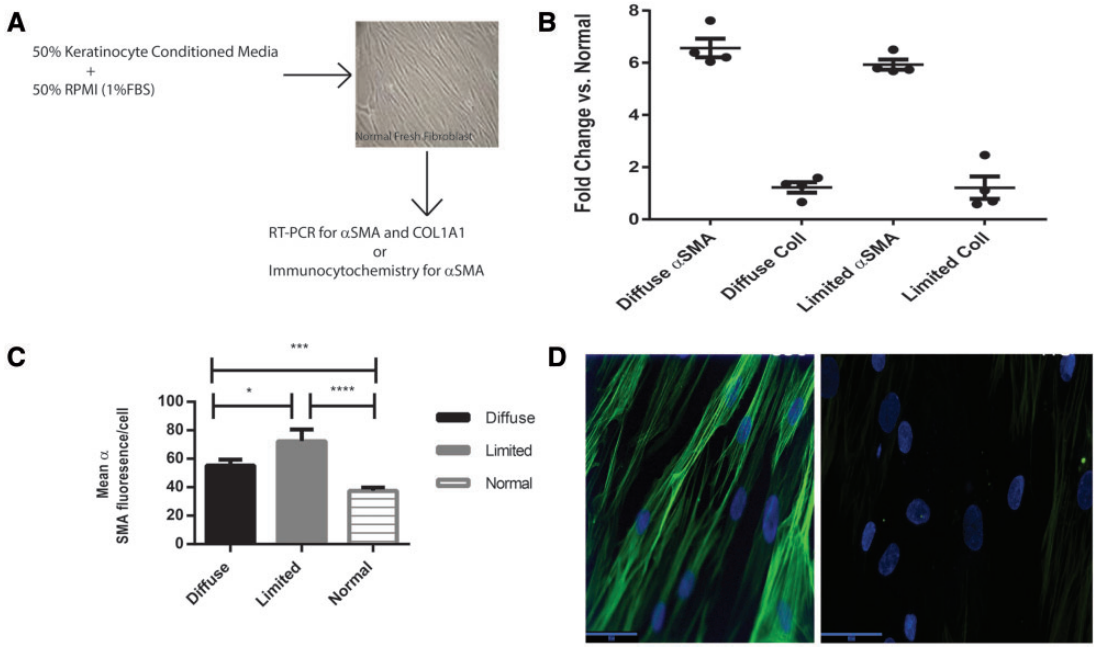

(**A**) Fresh fibroblasts were cultured with 50% keratinocyte conditioned media and 50% RPMI with 1% FBS for 24 h or 72 h and the cells were either harvested for RNA or fixed for immunocytochemistry. (**B**) Real-time PCR of fibroblasts stimulated with SSc or normal keratinocyte conditioned media for 24 h. Five lcSSc, five dcSSc and five normal samples were studied in triplicate on two separate fresh fibroblast cultures. Each dot represents the average of the triplicate. Error bars represent S.E.M.. α-SMA expression reported as a fold change compared with normal with significance ($P < 0.05$) calculated by comparison of ΔCTs via unpaired Student's *t*-test. (**C**) Immunocytochemistry of fibroblasts stimulated with SSc or normal keratinocyte conditioned media for 72 h. Three lcSSc, three dcSSc and five normal samples were studied in triplicate. Fibroblasts were fixed and stained with anti-α-SMA antibody and a secondary FITC-labelled antibody. Microscopy was performed and at least 20 images were taken per slide. α-SMA fluorescence was quantified with MetaMorph software as described in the Methods section. (**D**) Representative microscopy demonstrating α-SMA staining after exposure to SSc keratinocyte conditioned media (left) or normal keratinocyte conditioned media (right). Size bar = 50 mm. $^{*}P < 0.05$, $^{**}P < 0.01$, $^{***}P < 0.001$, $^{****}P < 0.0001$.

identified using Ingenuity Pathway Analysis software (www.ingenuity.com).

Statistical analysis

Results are expressed as mean (S.E.M.). Comparisons between two groups were made using a two-tiered unpaired Student's *t*-test. Correlations of real-time quantitative PCR gene expression data were completed via linear regression using GraphPad Prism software (GraphPad Software, La Jolla, CA, USA). *P*-values <0.05 were considered statistically significant.

Results

SSc keratinocyte conditioned media promotes transition of normal fibroblasts to myofibroblasts

Fibroblast activation, a central component of SSc, is characterized by COL1A1 and α-SMA expression [6]. Previous studies have demonstrated the presence of epidermal–dermal crosstalk as a possible contributing factor to SSc pathogenesis [13]. In order to establish the extent to which SSc keratinocytes may influence fibroblast activation, we incubated fresh fibroblasts from healthy subjects with conditioned media from SSc and normal patient keratinocytes. After 24 h, fibroblasts were harvested in Tripure and real-time PCR was performed to assess for expression of COL1A1 and α-SMA (Fig. 1A). The experiment was replicated on two separate freshly isolated primary fibroblast cultures. Fresh fibroblasts were found to have a significant increase in COL1A1 and α-SMA expression when treated with SSc keratinocyte conditioned media compared with normal keratinocyte conditioned media (Fig. 1B–D). These data suggest that SSc keratinocytes secrete pro-fibrotic factors that contribute to fibroblast activation.

Keratinocyte-mediated fibroblast activation is independent of TGF-β

TGF-β is considered central to fibroblast activation and fibrosis in SSc patients [19–21], thus we investigated

whether keratinocyte-derived TGF-β was driving fibroblast activation in SSc. Paraffin-imbedded slides were stained with TGF-β. Microscopy was performed and the mean immunofluorescence/area was calculated using MetaMorph. We found no significant difference between TGF-β expression in lcSSc, dcSSc or normal epidermis (Fig. 2A and B). TGF-β expression was increased in dcSSc dermis compared with epidermis consistent with previous reports [22]. We were unable to detect TGF-β secretion from SSc keratinocytes by ELISA (data not shown). To confirm that TGF-β was not responsible for keratinocyte-mediated fibroblast activation, a TGF-β neutralizing antibody was then added to fresh fibroblasts prior to stimulation with keratinocyte conditioned media. Immunofluorescence microscopy was performed 72 h later. No difference in fibroblast α-SMA expression was seen with TGF-β neutralization (Fig. 2C). The efficacy of the neutralizing antibody was confirmed with control experiments showing a significant reduction in α-SMA expression after stimulation with rhTGF-β in cells pretreated with TGF-β neutralizing antibody (Fig. 2D). These data confirm that while SSc keratinocytes can activate myofibroblast transformation, this effect is independent of TGF-β.

Transcriptomic comparison of SSc and normal keratinocytes identifies NF-κB activation and PPAR-γ repression as common changes in lcSSc and dcSSc keratinocytes

In order to capture differential expression changes and identify other pathways that may contribute to fibroblast activation by SSc keratinocytes, comparison of transcriptional profiles from seven lcSSc, five dcSSc and seven normal samples was completed using strict criteria ($q < 0.01$ and a fold change $\geqslant 1.5$ for upregulated genes and $\leqslant 0.6$ for downregulated genes). The top 20 up- and downregulated genes in dcSSc and lcSSc compared with normal keratinocytes are highlighted in supplementary Table S3, available at *Rheumatology* Online. As both dcSSc and lcSSc keratinocytes demonstrate fibroblast activation, we focused on their common molecular signature to identify potential contributors to this phenotype. The Genomatix Pathway System highlighted major nodes regulated in both dcSSc and lcSSc that included the transcription factors NF-κB1 (upregulated) and PPAR-γ (downregulated) (Fig. 3). Transcription factor analysis showed that the list of genes commonly differentially regulated in both diseases was enriched in genes having potential binding sites in their promoter for NF-κB1 and PPAR-γ (supplementary Table S4, available at *Rheumatology* Online and Table 1). Ingenuity Pathway Analysis software identified canonical pathways involved in both dcSSc and lcSSc, including eukaryotic initiation factor 2 (EIF2) signalling, L-cysteine degradation II and pyrimidine ribonucleotides interconversion (Table 2). Upstream regulator analysis identified a significant link between thioredoxin interacting protein, which is upregulated in both dcSSc and lcSSc, and activation of NF-κB, suggesting a possible role for oxidative stress in upregulation of NF-κB in SSc (supplementary Table S5, available at *Rheumatology* Online).

Unique transcriptomic features of dcSSc and lcSSc

Major nodes unique to dcSSc *vs* normal were downregulated and included TGF-β1, MMP2 and IL-1β (Fig. 3). Major nodes unique to lcSSc compared with normal were upregulated and included CCL2, MMP1 and 3, FGF2, RUNX2 and COL1A1. Top transcription factors identified in dcSSc compared with normal were SMAD4, JUNB, STAT2 and IRF9, while RUNX2 and KLF4 were identified in lcSSc (supplementary Table S4, available at *Rheumatology* Online).

CCL5 is increased in SSc keratinocytes

Real-time PCR confirmed upregulation of NF-κB1 in SSc keratinocytes and no significant change in PPAR-γ or TGF-β in SSc compared with control keratinocytes (Fig. 4A). As PPAR-γ and NF-κB have been noted to be opposing regulators of CCL5 [23], a chemokine with strong links to scleroderma pathogenesis [24], we evaluated expression of CCL5 and two other NF-κB-regulated cytokines, IL-6 and TNF-α, in SSc keratinocytes via real-time PCR. Consistent with a pattern of NF-κB activation and PPAR-γ inhibition, all three cytokines were upregulated in SSc keratinocytes as compared with controls (Fig. 4A). Importantly, there was a strong correlation between NF-κB upregulation and all three examined NF-κB-regulated genes ($P = 0.004$, $R^2 = 0.718$ for *CCL5*; $P = 0.004$, $R^2 = 0.725$ for *TNFAI*; $P = 0.024$, $R^2 = 0.540$ for *IL6*) but not for *TGFB1* ($P = 0.152$, $R^2 = 0.269$) (Fig. 4B). Expression of NF-κB and its regulated genes also correlated with patients' MRSS (Fig. 4C). Further support for the imbalance of NF-κB and PPAR-γ was noted through immunohistochemistry, which identified increased CCL5 expression in basal keratinocytes of SSc skin biopsies but minimal CCL5 staining in healthy control epidermis (Fig. 4D). Together these data support a functional dysregulation of cytokines positively regulated by NF-κB and negatively regulated by PPAR-γ in SSc keratinocytes.

Discussion

SSc is a disease associated with significant morbidity and mortality but lacks clear biomarkers or defined therapeutic targets. In this study we demonstrate that lcSSc- and dcSSc-derived keratinocytes have pro-fibrotic effects on normal primary fibroblasts as manifested by *ASMA* and *COL1A1* mRNA and protein expression. This pro-fibrotic effect is not related to keratinocyte production of TGF-β. Expression analysis of SSc and normal keratinocytes identified NF-κB and PPAR-γ as commonly, and oppositely, dysregulated nodes in both lcSSc and dcSSc, indicating that inhibition of NF-κB or downstream cytokines or activation of PPAR-γ may have therapeutic benefits in SSc.

Crosstalk between keratinocytes and the dermis has recently come under investigation [13]. Although SSc fibroblasts have received attention in the scientific

Fig. 2 Keratinocyte-induced myofibroblast transformation is independent of TGF-β

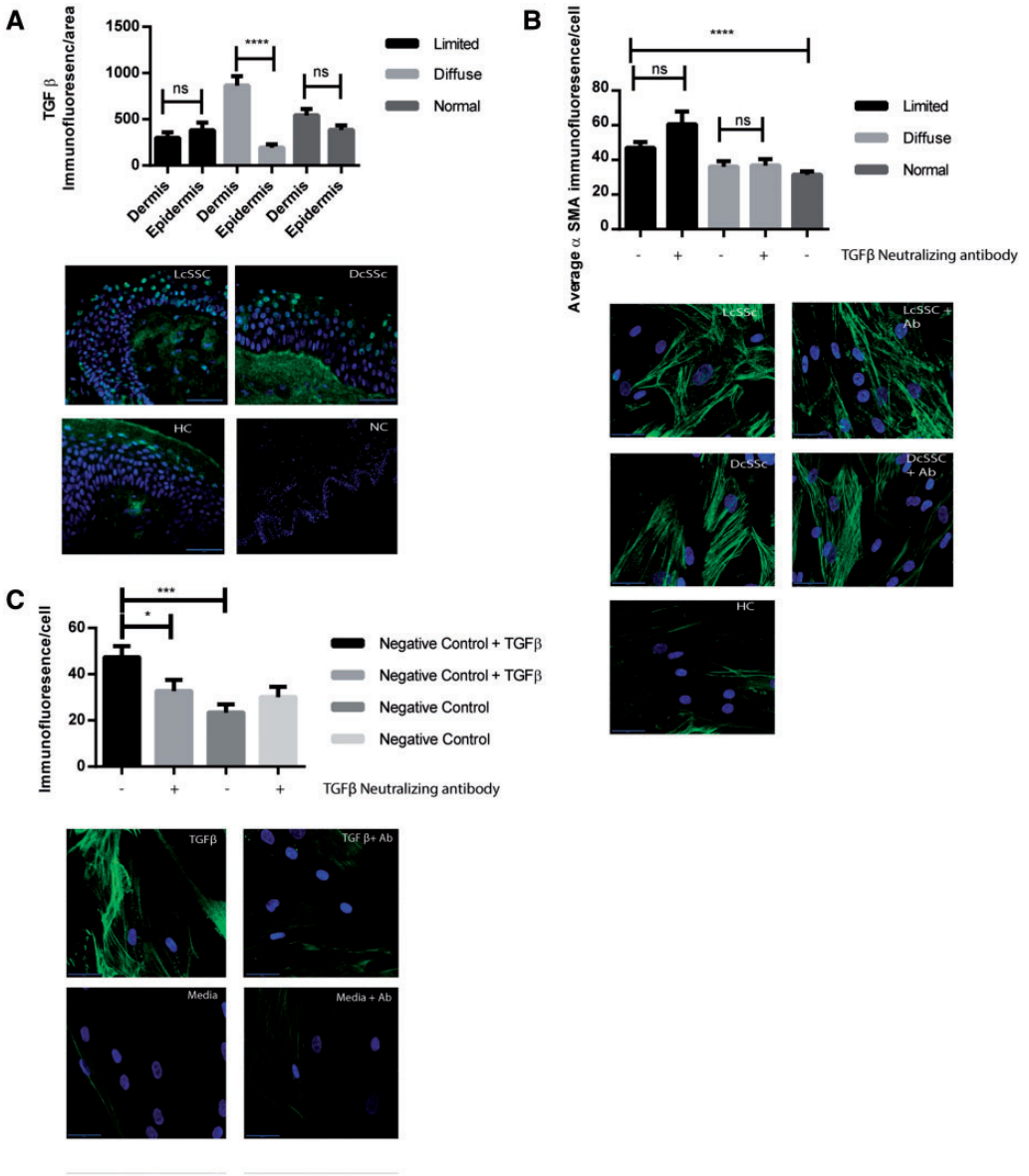

(**A**) Immunocytochemistry of TGF-β expression of three lcSSc, four dcSSc and four normal skin samples in triplicate demonstrate that there was no difference between dermis and epidermis in limited and normal samples. Greater TGF-β expression was seen in dcSSc dermis compared with epidermis. Representative biopsies of limited (upper left), diffuse (upper right), normal slides (lower left) and negative isotype control (lower right) stained with TGF-β. (**B**) Fibroblasts were incubated with normal or SSc conditioned media for 24 h with and without a neutralizing TGF-β antibody (two lcSSc, two dcSSc and three normal, in triplicate). At least 20 images were taken per slide using fluorescent microscopy. α-SMA expression was quantified with MetaMorph software as described in the Methods section. Representative images of fibroblasts stained for α-SMA are shown: lcSSc fibroblast α-SMA expression (upper left), lcSSc fibroblast + TGF-β neutralizing antibody (upper right), dcSSc fibroblast α-SMA expression (middle left), dcSSc fibroblast + TGF-β neutralizing antibody (middle right) and healthy control (bottom). (**C**) To validate the efficacy of our neutralizing antibody, fibroblasts were incubated with 10 ng/ml rhTGF-β in the presence or absence of TGF-β neutralizing antibody and α-SMA expression was evaluated as in (B). Representative images of normal fibroblasts treated with rhTGF-β and TGF-β neutralizing antibody (Ab) stained for α-SMA incubated in normal culture media are shown: stimulated with rhTGF-β (upper left), treated with rhTGF-β and TGF-β neutralizing Ab (upper right), negative control (lower left) and negative control treated with TGF-β neutralizing Ab (lower right). Size bar = 50 mm. $^{*}P < 0.05$, $^{**}P < 0.01$, $^{***}P < 0.001$, $^{****}P < 0.0001$.

Fig. 3 Transcriptional networks from dcSSc and lcSSc identify overlapping and unique pathways

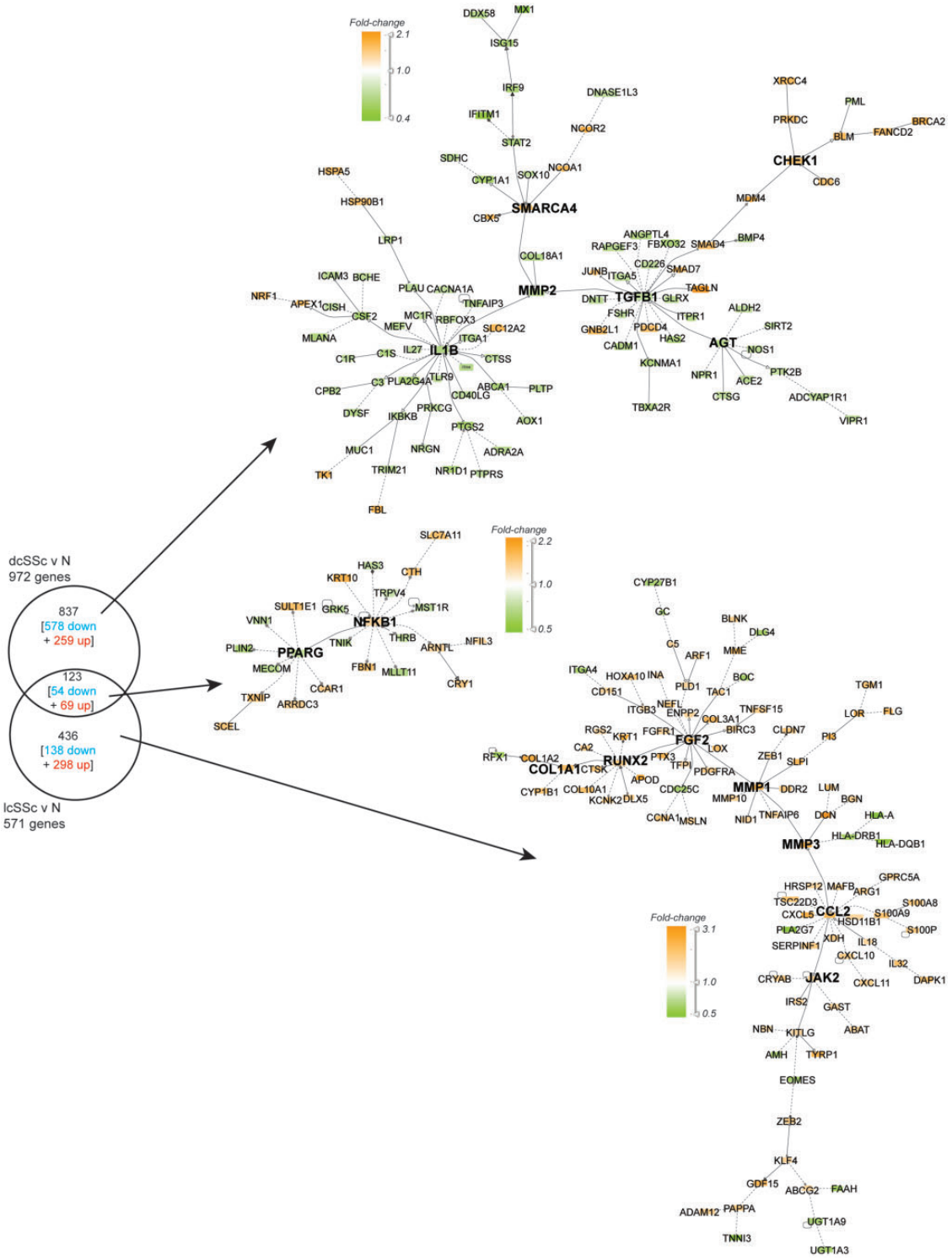

There were 123 genes regulated in the same direction in the 135 genes commonly regulated in both diseases. The pictures display the 100 best-connected genes (most relevant genes/interactions) co-cited in PubMed abstracts in the same sentence linked to a function word (e.g. gene A activates gene B). Orange represents the genes that are upregulated and green represents the genes that are downregulated in disease compared with normal.

Table 1 Transcription factor binding site analysis for commonly regulated genes in lcSSc and dcSSc

Gene	Name	Fold change in dcSSc *vs* normal	Fold change in lcSSc *vs* normal
27 genes (22% having a potential binding site for NF-κB1 (V$NFKB) in their promoter)			
ATRX	Alpha thalassemia/mental retardation syndrome X-linked	1.64	1.63
SEC16A	SEC16 homolog A (*S. cerevisiae*)	1.66	1.53
MUC16	Mucin 16, cell surface associated	0.66	0.64
TXNIP	Thioredoxin interacting protein	1.86	1.69
CTH	Cystathionine gamma-lyase	1.87	1.61
THRB	Thyroid hormone receptor beta	0.60	0.64
MLLT11	Myeloid/lymphoid or mixed-lineage leukaemia (trithorax homolog, Drosophila); translocated to, 11	0.56	0.52
PPARG	Peroxisome proliferator-activated receptor gamma	0.61	0.65
PLIN2	Perilipin 2	0.52	0.62
MST1R	Macrophage stimulating 1 receptor (c-met-related tyrosine kinase)	0.62	0.64
ARNTL	Aryl hydrocarbon receptor nuclear translocator-like	1.53	1.52
DSG1	Desmoglein 1	1.92	2.50
TNIK	TRAF2 and NCK interacting kinase	0.59	0.63
GRK5	G protein-coupled receptor kinase 5	0.60	0.64
SPINK5	Serine peptidase inhibitor, Kazal type 5	1.78	2.07
MECOM	MDS1 and EVI1 complex locus	0.57	0.58
UGT1A6	UDP glucuronosyltransferase 1 family, polypeptide A6	0.55	0.63
CRY1	Cryptochrome circadian clock 1	1.68	1.53
VNN1	Vanin 1	0.63	0.63
TRPV4	Transient receptor potential cation channel, subfamily V, member 4	0.65	0.66
PARP4	Poly (ADP-ribose) polymerase family, member 4	1.58	1.62
REV3L	REV3-like, polymerase (DNA directed), zeta, catalytic subunit	1.55	1.52
FBN1	Fibrillin 1	1.85	1.96
AGTPBP1	ATP/GTP binding protein 1	1.71	1.55
NFIL3	Nuclear factor, interleukin 3 regulated	1.57	1.56
NFKB1	Nuclear factor of kappa light polypeptide gene enhancer in B-cells 1	1.54	1.52
HAS3	Hyaluronan synthase 3	0.63	0.64
17 genes (13.8% having a potential binding site for PPAR-γ (V$PPAR, V$PERO) in their promoter			
NFKB1	Nuclear factor of kappa light polypeptide gene enhancer in B-cells 1	1.54	1.52
TXNIP	Thioredoxin interacting protein	1.86	1.69
CCAR1	Cell division cycle and apoptosis regulator 1	1.65	1.59
THRB	Thyroid hormone receptor, beta	0.60	0.64
ARRDC3	Arrestin domain containing 3	1.61	1.74
PLIN2	Perilipin 2	0.52	0.62
ARNTL	Aryl hydrocarbon receptor nuclear translocator-like	1.53	1.52
SULT1E1	Sulfotransferase family 1E, estrogen-preferring, member 1	1.89	1.89
GRB14	Growth factor receptor-bound protein 14	0.64	0.64
SPINK5	Serine peptidase inhibitor, Kazal type 5	1.78	2.07
MECOM	MDS1 and EVI1 complex locus	0.57	0.58
UGT1A6	UDP glucuronosyltransferase 1 family, polypeptide A6	0.55	0.63
CRY1	Cryptochrome circadian clock 1	1.68	1.53
VNN1	vanin 1	0.63	0.63
TRPV4	Transient receptor potential cation channel, subfamily V, member 4	0.65	0.66
PARP4	Poly (ADP-ribose) polymerase family, member 4	1.58	1.62
NFIL3	Nuclear factor, interleukin 3 regulated	1.57	1.56

literature, few studies have focused on the SSc keratinocyte. Aden *et al.* [25] demonstrated that incubation of whole epidermis of SSc patients could promote contraction of fibroblast-populated collagen lattices. This process was antagonized by IL-1RA and possibly mediated by S100A9. Our data, which analyse the contributions of a pure primary keratinocyte population from SSc skin, support this study and describe a role for this specific cell population in pro-fibrotic effects.

Past studies have demonstrated conflicting results regarding expression of TGF-β in the epidermis. One study demonstrated increased immunofluorescence staining of TGF-β in dcSSc epidermis compared with control epidermis. However, this analysis was performed with a subjective grading scale [26]. In contrast, another study demonstrated no difference in TGF-β production by ELISA in normal and dcSSc whole epidermis [27]. We did not detect TGF-β production by SSc keratinocytes

Table 2 Ingenuity pathway analysis of genes regulated in the same direction in lcSSc and dcSSc

Canonical pathways (number of genes regulated in the pathway/number of genes in the pathway)	*P*-value	Regulated molecules in the pathway
EIF2 signalling (5/163)	3.80E-03	RPL5, RPL7A, RPL21, RPS2, EIF4G2
L-cysteine degradation II (1/1)	6.31E-03	CTH
Pyrimidine ribonucleotides interconversion (2/25)	1.10E-02	AK5, ENTPD3
IL-15 production (2/27)	1.26E-02	NF-κB1, MST1R
Pyrimidine ribonucleotides *de novo* biosynthesis (2/27)	1.26E-02	AK5, ENTPD3
Cysteine Biosynthesis/homocysteine degradation (1/2)	1.26E-02	CTH
Circadian rhythm signalling (2/32)	1.74E-02	ARNTL, CRY1
NAD biosynthesis from 2-amino-3-carboxymuconate semialdehyde (1/6)	3.72E-02	QPRT
Wnt/Ca^+ pathway (2/53)	4.47E-02	NF-κ B1, PLCB4
IL-12 signalling and production in macrophages (3/126)	4.57E-02	NF-κ B1, MST1R, PPAR-γ
Adipogenesis pathway (3/128)	4.79E-02	ARNTL, TXNIP, PPAR-γ

basally or with TLR stimulation, and our data suggest that TGF-β does not participate in pro-fibrotic epidermal–dermal crosstalk despite its importance in the pro-fibrotic process [19, 20, 28]. This is particularly pertinent given recent data that fresolimumab, an anti-TGF-β antibody, decreases expression of TGF-β biomarker genes and decreases MRSS in a small sample of early dcSSc patients [29]. Our data would suggest that anti-TGF-β therapy might not be as robust a candidate for possible topical application.

Commonly regulated pathways in both dcSSc and lcSSc keratinocytes likely are responsible for the promotion of fibrosis by keratinocytes in both subsets. Through microarray, we were able to identify two interesting targets for future study. NF-κB1 and PPAR-γ were commonly upregulated and downregulated in dcSSc and lcSSc keratinocytes, respectively. NF-κB is a ubiquitous transcription factor that plays an integral role in inflammation, immune system regulation and autoimmunity and has been identified in genome-wide association studies to be a probable SSc risk factor [30]. c-Rel, a subunit of NF-κB, has been implicated in fibrosis in cardiac and liver studies [31, 32]. Interestingly, NF-κB1 knockout mice are not protected from bleomycin-induced skin injury, but this does preclude inflammatory signalling downstream of NF-κB1 activation from having pro-fibrotic effects in humans [12]. PPAR-γ is a ligand-dependent nuclear receptor that has anti-fibrotic effects when activated. Importantly, a variant of PPAR-γ has been associated with SSc [33], and *in vivo* studies of a PPAR-γ agonist demonstrate diminished skin fibrosis [34]. PPAR-γ knockout mice have increased susceptibility to bleomycin-induced fibrosis [35], suggesting that the repression of PPAR-γ in SSc keratinocytes may also promote pro-fibrotic effects. Importantly, PPAR-γ activation can repress NF-κB-induced inflammation in the skin [36]. This suggests that the interaction between these two transcription factors may be a central regulatory mechanism by which SSc keratinocytes can promote fibrosis.

CCL5, a chemokine that is known to be positively regulated by NF-κB and negatively regulated by PPAR-γ, has been linked to SSc in the skin [37] and peripheral blood [38, 39]. CCL5 is stimulated by pro-inflammatory markers such as TNF and IL-1β [40] and can subsequently lead to production of IL-6 [41], a cytokine associated with the extent of skin disease in SSc [42] and one we found was also upregulated in SSc keratinocytes. Furthermore, CCL5 has been implicated in a single-nucleotide polymorphism (SNP)–SNP interaction that may increase the risk of SSc development [24]. Blockade of the CCL5 receptors CCR1 and CCR5 suppresses renal fibrosis and bleomycin-induced pulmonary fibrosis, respectively [43, 44]. Thus we propose that SSc keratinocytes have decreased expression of PPAR-γ, leading to increased NF-κB1 and subsequent CCL5 production, which may lead to pro-fibrotic effects on fibroblasts. We acknowledge that other factors, not detectable by microarray, including lipid mediators, prostaglandins and some microRNAs may also be playing a role in keratinocyte–fibroblast crosstalk.

Of note, we found a general repression of type I IFN-regulated transcripts in both lcSSc and dcSSc keratinocytes. The role of type I IFN may be cell specific in SSc skin. Type I IFN-regulated genes are increased in SSc biopsies, especially in association with endothelial cells and vascular dysfunction in this disease [45, 46]. Whole skin biopsies have shown type I IFN gene upregulation to be associated with macrophage-associated genes [47]. Intriguingly, like our data, single-cell analysis of fibroblasts shows repression of type I IFN-regulated genes [48]. In both dcSSc and lcSSc patients we see a general repression of IFN-κ, a keratinocyte-specific type I IFN important for cutaneous lupus [49], and this may be one mechanism by which type I IFN signatures are decreased in SSc keratinocytes. Interestingly, previous global whole skin expression studies in SSc patients have demonstrated increased keratin transcripts [50]. We also noted increased keratin expression in both lcSSc and dcSSc samples. Assassi *et al.* [50] speculate that an upregulated keratin signature reflects upstream activation of the Wnt/β-catenin signalling, providing another possible target for future investigation.

Fig. 4 NF-κB-regulated cytokines are increased in SSc keratinocytes

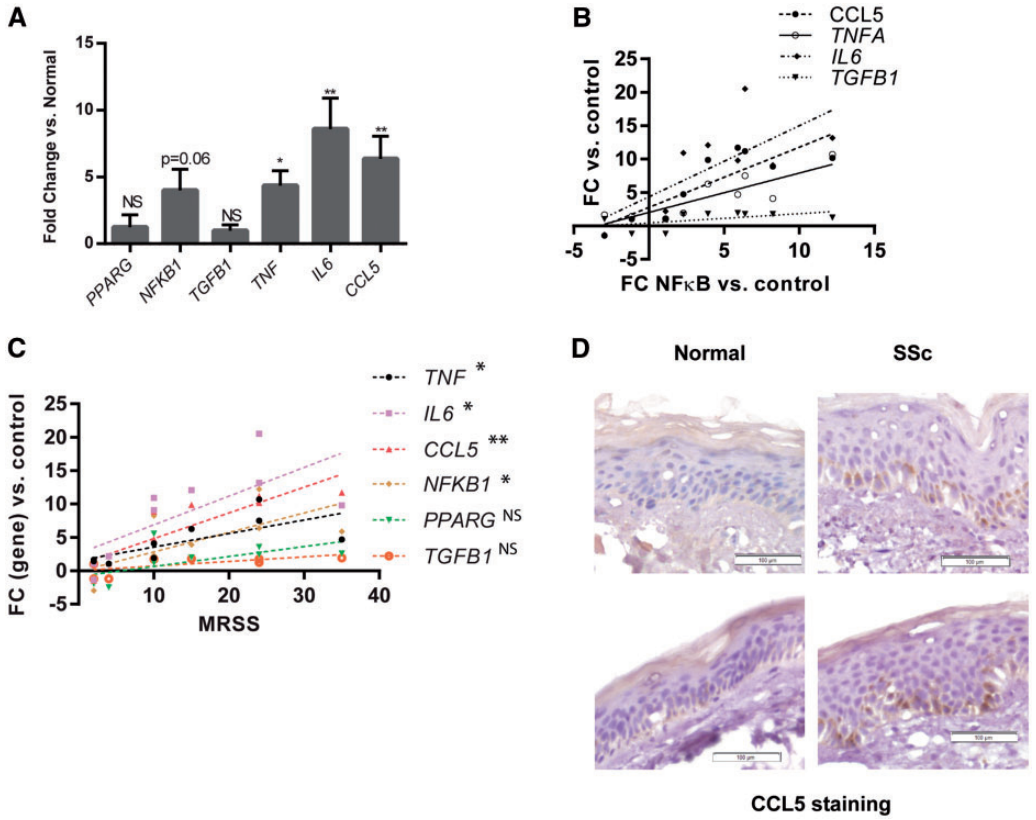

(**A**) Real-time PCR was completed on RNA from nine SSc and five healthy control keratinocyte cultures for the indicated genes. Data are expressed as fold change (FC) in the SSc sample *vs* the average of healthy controls. Graphs represent the mean (S.E.M.). Significance was analysed via Student's unpaired *t*-test. $^{*}P < 0.05$, $^{**}P < 0.01$. (**B**) FCs of indicated genes were plotted *vs* the FC of NF-κB and linear regression was completed (indicated lines). (**D**) FCs of indicated genes were plotted *vs* MRSS for each patient. Linear regression was performed. $^{*}P < 0.05$, $^{**}P < 0.01$. NS, not significant. (**C**) Representative CCL5 immunohistochemistry from three healthy controls and seven SSc patients. Scale bar = 100 μm.

Our data provide compelling evidence that keratinocytes are involved in the pathogenesis of SSc and that fibroblast activation by keratinocytes does not involve TGF-β. Abnormal regulation of PPAR-γ and NF-κB pathways may be central to the promotion of keratinocyte-induced fibroblast activation through CCL5 and additional downstream cytokines.

Acknowledgements

The authors would like to acknowledge the following people and cores for their vital role in this manuscript: University of Michigan DNA Sequencing Core, O'Brien Kidney Research Core Center (P30DK081943), Phillip L. Campbell, and the patients of the University of Michigan Scleroderma Program. P.S.T. received support from T32AR007080 and the Scleroderma Foundation. S.S.M. was supported by the US Department of Veterans Affairs.

Funding: Research reported in this publication was supported by the National Center for Advancing Translational Sciences of the National Institutes of Health under award number UL1TR000433 (subproject) and by the National Institute of Arthritis and Musculoskeletal and Skin Diseases of the National Institutes of Health under award numbers K08AR063668 and K24AR063120. The content of this article is solely the responsibility of the authors and does not necessarily represent the official views of the National Institutes of Health.

Disclosure statement: D.K. was funded by K24 National Institutes of Health/National Institute of Arthritis and Musculoskeletal and Skin Diseases AR063120, has received investigator-initiated grants and acts as a consultant to Actelion, Bristol-Myers Squibb, Bayer, Corbus, Cytori, ChemoMab, GlaxoSmithKline, Genentech/Roche and Sanofi-Aventis. All other authors have declared no conflicts of interest.

Supplementary data

Supplementary data are available at *Rheumatology* Online.

References

1 Lawrence RC, Helmick CG, Arnett FC *et al*. Estimates of the prevalence of arthritis and selected musculoskeletal disorders in the United States. Arthritis Rheum 1998;41:778–99.

2 Chifflot H, Fautrel B, Sordet C, Chatelus E, Sibilia J. Incidence and prevalence of systemic sclerosis: a systematic literature review. Semin Arthritis Rheum 2008;37:223–35.

3 Al-Dhaher FF, Pope JE, Ouimet JM. Determinants of morbidity and mortality of systemic sclerosis in Canada. Semin Arthritis Rheum 2010;39:269–77.

4 Shand L, Lunt M, Nihtyanova S *et al*. Relationship between change in skin score and disease outcome in diffuse cutaneous systemic sclerosis: application of a latent linear trajectory model. Arthritis Rheum 2007;56:2422–31.

5 Wynn TA. Common and unique mechanisms regulate fibrosis in various fibroproliferative diseases. J Clin Invest 2007;117:524–9.

6 Gabbiani G. The myofibroblast in wound healing and fibrocontractive diseases. J Pathol 2003;200:500–3.

7 Varga J, Pasche B. Antitransforming growth factor-beta therapy in fibrosis: recent progress and implications for systemic sclerosis. Curr Opin Rheumatol 2008;20:720–8.

8 Wynn TA, Ramalingam TR. Mechanisms of fibrosis: therapeutic translation for fibrotic disease. Nat Med 2012;18:1028–40.

9 Maurer B, Distler A, Suliman YA *et al*. Vascular endothelial growth factor aggravates fibrosis and vasculopathy in experimental models of systemic sclerosis. Ann Rheum Dis 2014;73:1880–7.

10 Aoudjehane L, Pissaia A Jr, Scatton O *et al*. Interleukin-4 induces the activation and collagen production of cultured human intrahepatic fibroblasts via the STAT-6 pathway. Lab Invest 2008;88:973–85.

11 Bhattacharyya S, Kelley K, Melichian DS *et al*. Toll-like receptor 4 signaling augments transforming growth factor-beta responses: a novel mechanism for maintaining and amplifying fibrosis in scleroderma. Am J Pathol 2013;182:192–205.

12 Fullard N, Moles A, O'Reilly S *et al*. The c-Rel subunit of NF-κB regulates epidermal homeostasis and promotes skin fibrosis in mice. Am J Pathol 2013;182:2109–20.

13 Canady J, Arndt S, Karrer S, Bosserhoff AK. Increased KGF expression promotes fibroblast activation in a double paracrine manner resulting in cutaneous fibrosis. J Invest Dermatol 2013;133:647–57.

14 Dai C, Wang H, Sung S-SJ *et al*. Interferon alpha on NZM2328.Lc1R27: enhancing autoimmunity and immune complex-mediated glomerulonephritis without end stage renal failure. Clin Immunol 2014;154:66–71.

15 LeRoy EC, Black C, Fleischmajer R *et al*. Scleroderma (systemic sclerosis): classification, subsets and pathogenesis. J Rheumatol 1988;15:202–5.

16 Chen M, Huang J, Yang X *et al*. Serum starvation induced cell cycle synchronization facilitates human somatic cells reprogramming. PLoS One 2012;7:e28203.

17 Haak AJ, Tsou PS, Amin MA *et al*. Targeting the myofibroblast genetic switch: inhibitors of myocardin-related transcription factor/serum response factor-regulated gene transcription prevent fibrosis in a murine model of skin injury. J Pharmacol Exp Ther 2014;349:480–6.

18 Hodgin JB, Nair V, Zhang H *et al*. Identification of cross-species shared transcriptional networks of diabetic nephropathy in human and mouse glomeruli. Diabetes 2013;62:299–308.

19 Dong C, Zhu S, Wang T *et al*. Deficient Smad7 expression: a putative molecular defect in scleroderma. Proc Natl Acad Sci USA 2002;99:3908–13.

20 Leask A, Abraham DJ, Finlay DR *et al*. Dysregulation of transforming growth factor beta signaling in scleroderma: overexpression of endoglin in cutaneous scleroderma fibroblasts. Arthritis Rheum 2002;46:1857–65.

21 Cotton SA, Herrick AL, Jayson MI, Freemont AJ. TGF beta—a role in systemic sclerosis? J Pathol 1998;184:4–6.

22 Querfeld C, Eckes B, Huerkamp C, Krieg T, Sollberg S. Expression of TGF-β1, -β2 and -β3 in localized and systemic scleroderma. J Dermatol Sci 1999;21:13–22.

23 Solleti SK, Simon DM, Srisuma S, Arikan MC, Bhattacharya S. Airway epithelial cell PPARγ modulates cigarette smoke-induced chemokine expression and emphysema susceptibility in mice. Lung Cell Mol Physiol 2015;309:L293–304.

24 Lee EB, Zhao J, Kim JY, Xiong M, Song YW. Evidence of potential interaction of chemokine genes in susceptibility to systemic sclerosis. Arthritis Rheum 2007;56:2443–8.

25 Nikitorowicz-Buniak J, Shiwen X, Denton CP, Abraham D, Stratton R. Abnormally differentiating keratinocytes in the epidermis of systemic sclerosis patients show enhanced secretion of CCN2 and S100A9. J Invest Dermatol 2014;134:2693–702.

26 Rudnicka L, Varga J, Christiano AM *et al*. Elevated expression of type VII collagen in the skin of patients with systemic sclerosis. Regulation by transforming growth factor-beta. J Clin Invest 1994;93:1709–15.

27 Aden N, Nuttall A, Shiwen X *et al*. Epithelial cells promote fibroblast activation via IL-1α in systemic sclerosis. J Invest Dermatol 2010;130:2191–200.

28 Whitfield ML, Finlay DR, Murray JI *et al*. Systemic and cell type-specific gene expression patterns in scleroderma skin. Proc Natl Acad Sci USA 2003;100:12319–24.

29 Rice LM, Padilla CM, McLaughlin SR *et al*. Fresolimumab treatment decreases biomarkers and improves clinical symptoms in systemic sclerosis patients. J Clin Invest 2015;125:2795–807.

30 Martin JE, Broen JC, Carmona FD *et al*. Identification of CSK as a systemic sclerosis genetic risk factor through Genome Wide Association Study follow-up. Hum Mol Genet 2012;21:2825–35.

31 Gaspar-Pereira S, Fullard N, Townsend PA *et al*. The NF-κB subunit c-Rel stimulates cardiac hypertrophy and fibrosis. Am J Pathol 2012;180:929–39.

32 Gieling RG, Elsharkawy AM, Caamano JH *et al*. The c-Rel subunit of nuclear factor-κB regulates murine liver inflammation, wound-healing, and hepatocyte proliferation. Hepatology 2010;51:922–31.

33 Marangoni RG, Korman BD, Allanore Y *et al*. A candidate gene study reveals association between a variant of the Peroxisome Proliferator-Activated Receptor Gamma

(PPAR-γ) gene and systemic sclerosis. Arthritis Res Ther 2015;17:128.

34 Wei J, Zhu H, Komura K *et al*. A synthetic PPAR-γ agonist triterpenoid ameliorates experimental fibrosis: PPAR-γ-independent suppression of fibrotic responses. Ann Rheum Dis 2014;73:446–54.

35 Kapoor M, McCann M, Liu S *et al*. Loss of peroxisome proliferator-activated receptor gamma in mouse fibroblasts results in increased susceptibility to bleomycin-induced skin fibrosis. Arthritis Rheum 2009;60:2822–9.

36 Mastrofrancesco A, Kovacs D, Sarra M *et al*. Preclinical studies of a specific PPARγ modulator in the control of skin inflammation. J Invest Dermatol 2014;134:1001–11.

37 Distler O, Rinkes B, Hohenleutner U *et al*. Expression of RANTES in biopsies of skin and upper gastrointestinal tract from patients with systemic sclerosis. Rheumatol Int 1999;19:39–46.

38 Scala E, Pallotta S, Frezzolini A *et al*. Cytokine and chemokine levels in systemic sclerosis: relationship with cutaneous and internal organ involvement. Clin Exp Immunol 2004;138:540–6.

39 Bandinelli F, Del Rosso A, Gabrielli A *et al*. CCL2, CCL3 and CCL5 chemokines in systemic sclerosis: the correlation with SSc clinical features and the effect of prostaglandin E1 treatment. Clin Exp Rheumatol 2012;30:S44–9.

40 Ortiz BD, Krensky AM, Nelson PJ. Kinetics of transcription factors regulating the RANTES chemokine gene reveal a developmental switch in nuclear events during T-lymphocyte maturation. Mol Cell Biol 1996;16:202–10.

41 Nanki T, Nagasaka K, Hayashida K, Saita Y, Miyasaka N. Chemokines regulate IL-6 and IL-8 production by fibroblast-like synoviocytes from patients with rheumatoid arthritis. J Immunol 2001;167:5381–5.

42 Khan K, Xu S, Nihtyanova S *et al*. Clinical and pathological significance of interleukin 6 overexpression in systemic sclerosis. Ann Rheum Dis 2012;71:1235–42.

43 Anders HJ, Vielhauer V, Frink M *et al*. A chemokine receptor CCR-1 antagonist reduces renal fibrosis after unilateral ureter ligation. J Clin Invest 2002;109:251–9.

44 Ishida Y, Kimura A, Kondo T *et al*. Essential roles of the CC chemokine ligand 3-CC chemokine receptor 5 axis in bleomycin-induced pulmonary fibrosis through regulation of macrophage and fibrocyte infiltration. Am J Pathol 2007;170:843–54.

45 Fleming JN, Nash RA, McLeod DO *et al*. Capillary regeneration in scleroderma: stem cell therapy reverses phenotype? PLoS One 2008;3:e1452.

46 McMahan ZH, Wigley FM, Casciola-Rosen L. Risk of digital vascular events in scleroderma patients who have both anticentromere and anti-interferon-inducible protein 16 antibodies. Arthritis Care Res (Hoboken) 2017;69:922–926.

47 Rice LM, Ziemek J, Stratton EA *et al*. A longitudinal biomarker for the extent of skin disease in patients with diffuse cutaneous systemic sclerosis. Arthritis Rheumatol 2015;67:3004–15.

48 Lindahl GE, Stock CJ, Shi-Wen X *et al*. Microarray profiling reveals suppressed interferon stimulated gene program in fibroblasts from scleroderma-associated interstitial lung disease. Respir Res 2013;14:80.

49 Stannard JN, Reed TJ, Myers E *et al*. Lupus skin is primed for IL-6 inflammatory responses through a keratinocyte-mediated autocrine type I interferon loop. J Invest Dermatol 2017;137:115–22.

50 Assassi S, Swindell WR, Wu M *et al*. Dissecting the heterogeneity of skin gene expression patterns in systemic sclerosis. Arthritis Rheumatol 2015;67:3016–26.